The Influence of Combined Loading on Fatigue Crack Growth from Small Defects

M. Endo[1] and A.J. McEvily[2]

[1] Department of Mechanical Engineering, Fukuoka University, 8-19-1 Nanakuma, Jonan-ku, Fukuoka 814-0180, Japan, endo@fukuoka-u.ac.jp
[2] Department of Materials Science and Engineering and Institute of Materials Science, University of Connecticut, Storrs, CT, USA, mcevily@mail.ims.uconn.edu

ABSTRACT. *A basic equation of crack growth: $da/dN = A(\Delta K_{eff} - \Delta K_{effth})^2$, proposed by McEvily et al., was used for the evaluation of growth and threshold behaviors of small cracks initiated from small defects in combined loading fatigue. Here A is a material constant, a is the crack length, N is the number of cycles, ΔK_{eff} is the effective stress intensity factor range and ΔK_{effth} is its threshold value. In the detailed evaluation of the behavior of small fatigue cracks, the Kitagawa effect, the elastic-plastic behavior of cracks in biaxial stress fields and crack closure effects were taken into account. In-phase and out-of-phase combined tension and torsion fatigue tests were conducted using 0.37 % carbon steel (JIS S35C) specimens containing holes whose diameters were 100 μm, 200 μm and 500 μm. The direction of crack propagation, S-N curves and fatigue limits were found to be in agreement with the analyzed behavior.*

INTRODUCTION

Many engineering applications involve the use of components of complex shape, e.g., crankshafts in automobiles, which are often subjected to multiaxial, cyclic loading involving combinations of tension, bending and torsion. In order to evaluate the fatigue lifetimes and fatigue limits of such components, a knowledge of the behavior of small fatigue cracks is necessary, since a major portion of the total fatigue lifetime is spent in the propagation of small cracks. In addition, the boundary between propagation and non-propagation of small cracks separates the safe from the potentially unsafe fatigue regimes.

McEvily et al. [1] have proposed a constitutive equation of the crack growth rate, d*a*/d*N*. In this approach, the following three aspects are taken into consideration in the evaluation of the behavior of small fatigue cracks:

(1) In the short-crack regime, crack growth is often elastic-plastic in nature rather than linear-elastic because of a high ratio of the fatigue strength to the yield strength and the consequent large ratio of the plastic zone to the crack length.
(2) As pointed out by Kitagawa and Takahashi [2], in a range of extremely short cracks

the endurance limit rather than the threshold for macroscopic crack propagation is the controlling factor governing crack propagation (Kitagawa effect).
(3) Crack closure is a function of the crack length. In the wake of a crack of a few microns in length the crack closure level is zero, but as the crack grows to a length of a millimeter or so the crack closure level rises to that of a large crack.

The objective of this study is to modify the above basic equation taking these three factors into account and then to predict the fatigue lifetimes and thresholds of specimens containing a small crack or hole subjected to in-phase and out-of-phase combined tension and torsion loadings.

EXTENSION OF THE MCEVILY EQUATION

McEvily et al. [1] proposed the basic equation of fatigue crack growth law as

$$\frac{\mathrm{d}a}{\mathrm{d}N} = A(\Delta K_{\mathrm{eff}} - \Delta K_{\mathrm{effth}})^2 \tag{1}$$

where a is the crack length; N is the number of load cycles; A is a constant which depends upon the material and the environment; ΔK_{eff} is the effective range of stress intensity factor (SIF) given by $K_{\max} - K_{\mathrm{op}}$, where $K_{\max}$ is the maximum value of SIF in a cycle and K_{op} is the value of SIF at the crack opening level; and $\Delta K_{\mathrm{effth}}$ is the ΔK_{eff} at threshold level, a material constant. Equation 1 modified to deal with short fatigue crack growth within a LEFM framework is given as

$$\frac{\mathrm{d}a}{\mathrm{d}N} = AM^2 \tag{2}$$

where

$$M = \left[\sqrt{2\pi r_{\mathrm{e}} F} + Y\sqrt{\pi a F}\right]\Delta\sigma - (1 - e^{-k\lambda})(K_{\mathrm{opmax}} - K_{\min}) - \Delta K_{\mathrm{effth}} \tag{3}$$

In this equation, $\Delta\sigma$ is the range of applied stress; r_{e} is a material constant of the order of 1 μm, and is treated as an inherent crack length in order to deal with the Kitagawa effect; F, the modification factor of the crack length to include the elastic-plastic behavior of a crack; k is a material constant which determines the rate of crack closure development; Y is the geometrical crack-shape correction factor of the SIF, and is 0.73 for an semi-circular crack assumed herein; λ is the length of the newly formed fatigue crack measured from the tip of an initial crack or defect; K_{opmax} is the crack opening level for a macroscopic crack; and $K_{\min}$ is the minimum value of SIF in a cycle. In Eq. 3, the first term represents the crack driving force, D, and the second and third terms represent the crack resisting force, R. Therefore $M = D - R$ is the net driving

force for crack propagation. In this study it was assumed that the crack tip was closed in compression, and therefore in the analysis, the stress amplitude was used in place of $\Delta\sigma$ and K_{min} was set equal to zero.

The variations in normal stress, σ, and torsional shear stress, τ, in a shaft subjected to combined tension and torsion loading at R of -1 are expressed as

$$\sigma = \sigma_0 \sin \omega t \tag{4}$$

$$\tau = \tau_0 \sin(\omega t + \delta) \tag{5}$$

where σ_a and τ_a are the amplitudes of normal stress and torsional shear stress, ω is the angular velocity, t is the time and δ is the phase difference. Note that the principal axes remain fixed during loading cycles under in-phase ($\delta = 0^o$) combined axial and torsional loading, but if there is a phase difference between axial and torsional loads the principal axes will rotate. It is assumed in this paper that Mode I loading will dominantly control the propagation behavior of a crack though the crack tip undergoes actually a mixed mode deformation under out-of-phase loading. Based on this hypothesis, the crack driving force, D, in Eq. 3 is modified by assuming a surface crack present in a biaxial stress field as [3]

$$D = \left[\left(1 - \frac{\sigma_p}{\sigma_n} \right) \sqrt{2\pi r_e F_{biaxial}} + Y \sqrt{\pi a F_{biaxial}} \right] \sigma_n \tag{6}$$

where σ_n and σ_p are the principal stress amplitudes applied in the direction normal and parallel to the crack face, respectively, $F_{biaxial}$ is further modified from F in Eq. 3 in accord with the von Mises criterion by taking biaxial stress condition into account, and given in a generalized form as

$$F_{biaxial} = \frac{1}{2} \left(1 + \sec \frac{\pi \sigma_n}{2\sigma_Y} \sqrt{1 - \frac{\sigma_n}{\sigma_p} + \left(\frac{\sigma_n}{\sigma_p} \right)^2} \right) \tag{7}$$

where σ_Y is the yield strength obtained in a uniaxial tensile test.

In the present study, it is assumed that a crack will propagate as a Mode I crack in the direction where D has its largest value, termed hereafter as D_{max}. The propagation rate, da/dN, and the threshold level of a surface crack under multiaxial loading are then determined by the value of M calculated from D_{max}. An example of variations in D, which were calculated by putting the resultant principal stresses, σ_1 and σ_2, into σ_n and σ_p in Eqs. 6 and 7, is shown in Fig. 1. In this figure, the values of σ_1 and σ_2, and the angle of the first principal axis, θ_1, relative to specimen axis are also plotted. It is seen that the values of D and θ_1 change with ωt but the maximum value, D_{max}, appears periodically at the same angle in a cycle. The value of D_{max} is calculated based upon

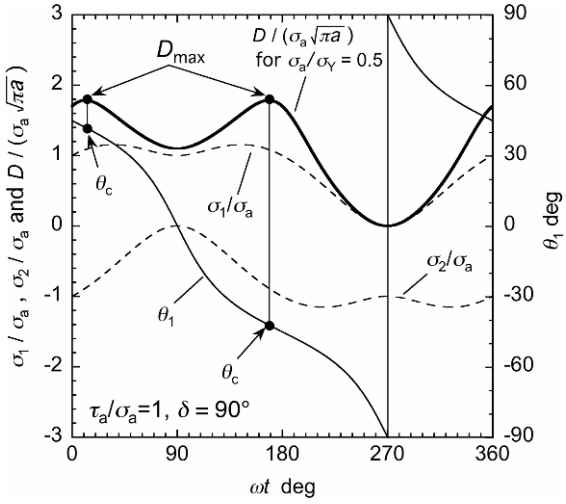

Figure 1. Variation of $D/(\sigma_0\sqrt{\pi a})$, σ_1/σ_a, σ_2/σ_a and θ_1 as a function of ωt.

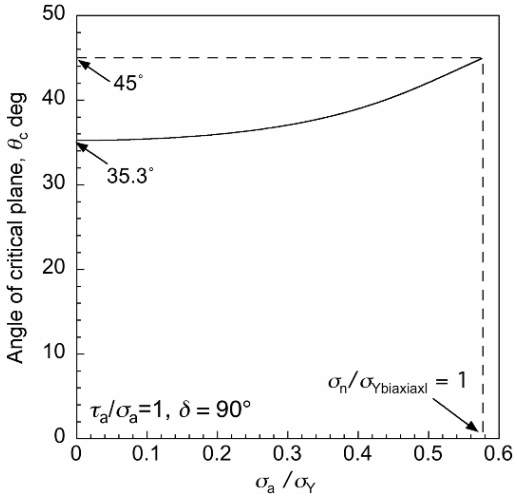

Figure 2. Angle of critical plane, θ_c, as a function of σ_a/σ_Y. $\sigma_{Ybiaxial}$ is the yield stress calculated based upon von Mises criterion.

Eqs. 6 and 7 and therefore the value of θ_1 corresponding to D_{max}, termed as θ_c, is not always constant for the same value of σ_n/σ_p but also depends on σ_n/σ_Y in Eq. 7. An example is shown in Fig. 2, in which θ_c is shown to be changed from 35.3 º to 45 º as a function of σ_a/σ_Y. It is expected that a crack will propagate on the plane determined by θ_c, considered a critical plane.

EXPERIMENTAL PROCEDURE

The material used in this investigation was a 0.37 % carbon steel (JIS S35C) which had been annealed at 860ºC for 1 h. The chemical composition and mechanical properties are shown in Tables 1 and 2. The microstructure is shown in Fig. 3.

Figure 4 shows the shape and dimensions of the test specimens. After machining, a 30 μm thick layer was removed from the surface by electro-polishing and then a small hole of the type shown in Fig. 4 was introduced into the surface by drilling. The diameter of the hole, d, was equal to the depth, h. Three hole sizes were used, 100 μm, 200 μm and 500 μm. All specimens were electro-polished after the drilling operation to remove a surface layer of 1-2 μm in thickness before fatigue testing. The equation used to treat a drilled hole as an equivalent semi-circular crack of half crack length, a_0, is given in Fig. 4.

A servo-hydraulic, uniaxial, fatigue testing machine operating at 40-55 Hz and a servo-hydraulic combined axial and torsional fatigue testing machine operating at 25-45 Hz were used. All fatigue tests were conducted under load-controlled, fully reversed (R = -1) sinusoidal loading. The following values of the ratio of the shear stress to the

normal stress, τ_a/σ_a, were used: 0, 1/2, 1, 2 and ∞. The phase differences, δ, were 0º and 90º ($\pi/2$ rad) between axial and torsional loads. The crack surface length was measured by the plastic replica method, and the value of da/dN was calculated using the secant method. The fatigue limit for the same ratio of τ_a/σ_a and the same phase difference was defined as the combination of the maximum normal stress amplitudes under which a specimen endured 10^7 cycles.

Table 1 Chemical composition (wt. %)

C	Si	Mn	P	S	Cu	Ni	Cr
0.37	0.21	0.65	0.019	0.017	0.13	0.06	0.14

Table 2 Mechanical properties

Yield strength MPa	Tensile strength MPa	Vickers hardness *HV*
328	586	160

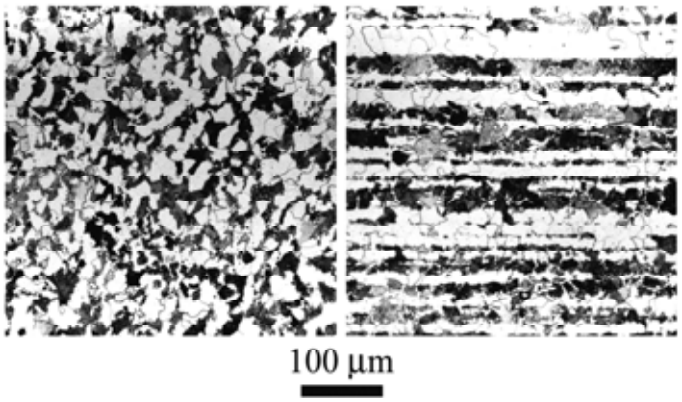

Figure 3. Microstructure: transverse section (*left*) and longitudinal section (*right*).

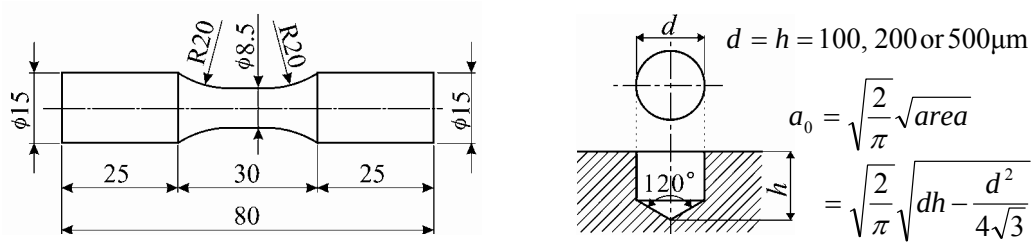

Figure 4. Shape and dimensions of smooth specimens and holes.

Table 3. Material constants used in the analysis

A $(\mathrm{MPa})^{-2}$	σ_{w0} MPa	K_{opmax} $\mathrm{MPa}\sqrt{\mathrm{m}}$	K_{effth} $\mathrm{MPa}\sqrt{\mathrm{m}}$	k m^{-1}	r_e μm
5.0×10^{-10}	230	3.3	3.0	6000	1.8

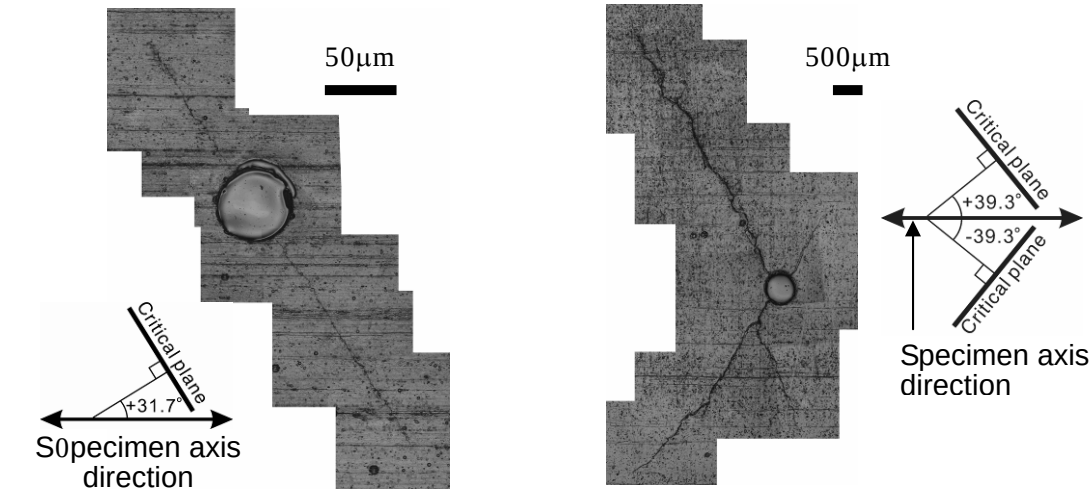

(a) In-phase loading, $\sigma_a = \tau_a = 100$ MPa, $\sigma_n / \sigma_Y = 0.49$, $\theta_c = 31.7^\circ$, $N_f = 1.65 \times 10^6$, Observation at $N = 1.57 \times 10^6$.

(b) 90º out-of-phase loading, $\sigma_a = \tau_a = 135$ MPa, $\sigma_n / \sigma_Y = 0.47$, $\theta_c = \pm 39.3^\circ$, $N_f = 6.4 \times 10^5$, Observation at $N = 6.2 \times 10^5$.

Figure 5. Cracks emanating from holes of $d = h = 500$ μm under in-phase and out-of-phase combined tension and torsion loadings.

RESULTS AND DISCUSSION

Figure 5 shows cracks that led to specimen fracture under in-phase and 90º out-of-phase loadings. The predicted directions of critical planes are also shown. The crack paths are microscopically irregular but macroscopically they are approximately on the critical planes. The width between crack faces is wider in Fig. 5b than in Fig. 5a presumably because of the abrasion of crack faces caused by shear mode loading.

Figure 6 shows the relationship between da/dN and M. The material constants used in the analysis are listed in Table 3, which are the same values as used in the previous analysis for the same material, JIS S35C, subjected to uniaxial loading. In the left figure, those values were used in the analyses for both in-phase and out-of-phase cases. It is seen that the data points for the out-of-phase case is a little higher than for the in-phase case. It is considered that this difference is due to the abrasion of crack surfaces which reduces the level of crack closure and thereby increased the net driving force. A best-fit line has been drawn through the data points obtained in the in-phase loading tests. The slope of this line is two in accord with Eq. 2. The value of A in Eq. 2 was determined to be 5×10^{-10} (MPa)$^{-2}$. In the right in Fig. 6, the smaller values of K_{opmax} and k were used for the out-of-phase case to consider the influence of crack face interference. Those values were used in the following analyses for the out-of-phase case.

The number of cycles to failure was calculated by integration of Eq. 2 between the limits of initial crack length, a_0, and the final crack length, a_f, assumed here to be 5 mm. In this calculation, the number of cycles spent in crack initiation is ignored and an initial

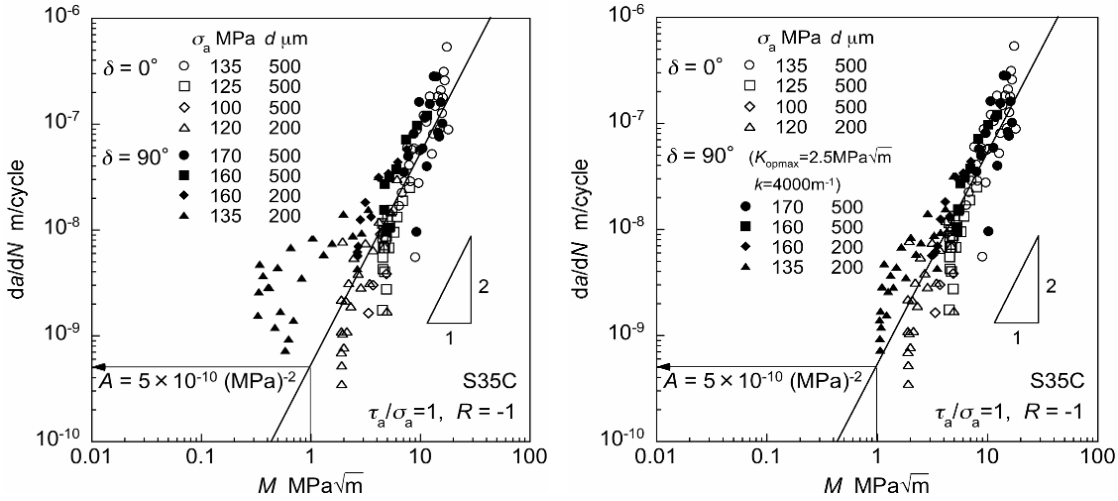

Figure 6. Relationship between da/dN and M. Reduction in crack closure level due to crack face interference for out-of-phase case is not considered in the left figure, whereas in the right figure, it is considered.

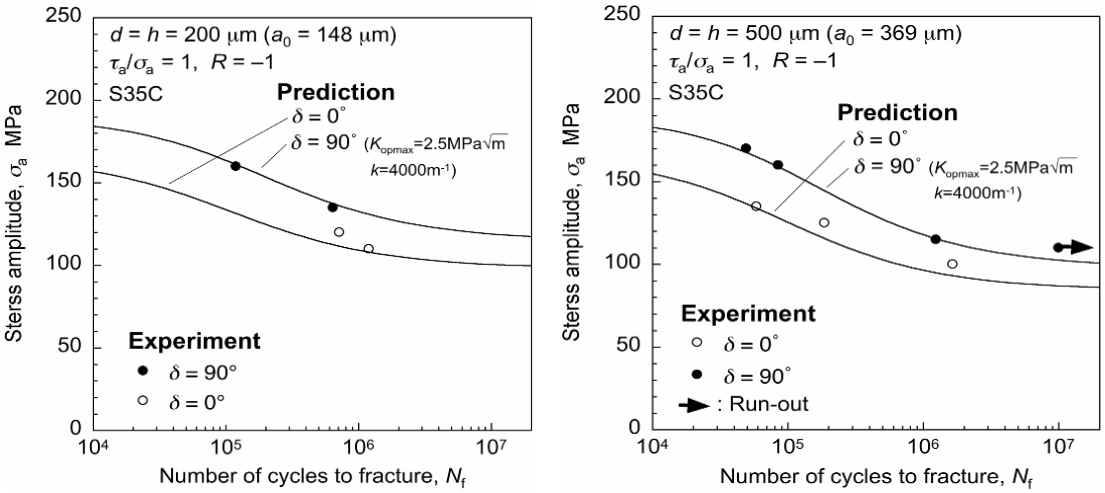

Figure 7. A comparison of predicted and experimental S-N curves. Reduction in crack closure level is considered for the out-of-phase case.

hole is regarded as an equivalent planar crack. The calculated S-N curves are shown in Fig. 7, together with the corresponding experimental results. Agreement between experimental and predicted results is good.

The fatigue limit of specimens can be predicted considering the threshold condition for propagation of a crack emanating from a hole. The minimum stress amplitude, σ_{th}, required to continue the propagation of a crack can be calculated by setting $M = 0$. In the calculation, the stress to propagate crack is determined as a function of λ, starting from an initial crack size of a_0. The fatigue limit for a given a_0 then corresponds to the maximum value of the calculated stress amplitude. This procedure is explained in more

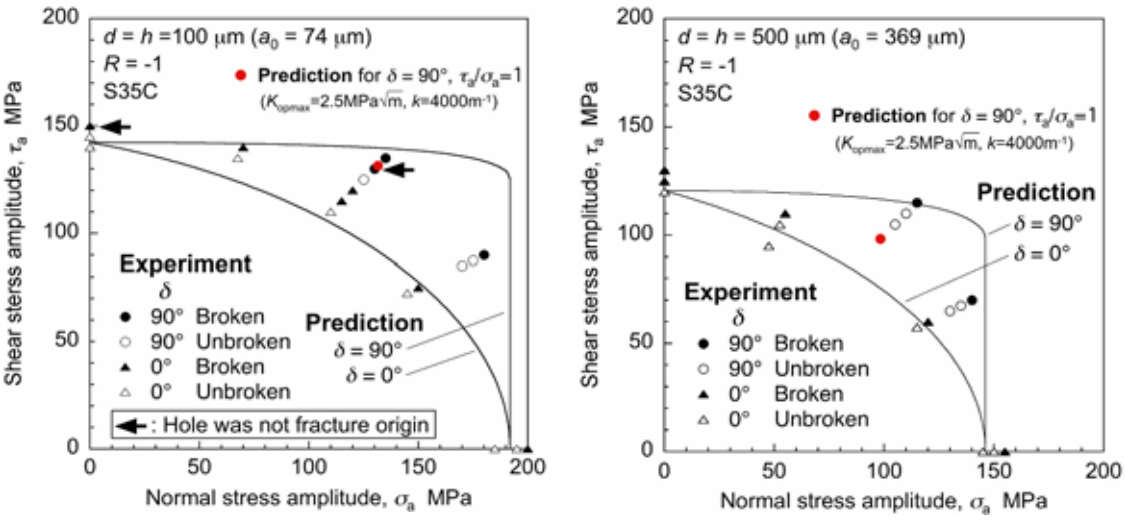

Figure 8. A comparison of prediction of fatigue limits with experimental results for different hole diameters of 100 μm (*left*) and 500μm (*right*).

detail in Ref. [3]. Figure 8 shows a comparison of the predicted fatigue limits with the experimental results performed at an R of –1 under in-phase and 90º out-of-phase combined loadings. It is of interest that in two instances indicated by the arrows in Fig. 8a, the 100 μm holes were so innocuous that failure initiated away from the holes. In all other cases, the fatigue strength was determined by holes. It is seen that the experimental data for the fatigue limits and the predicted values are in reasonable agreement.

CONCLUDING REMARKS

In this study the equation proposed by McEvily has been extended to deal with fatigue crack propagation under complex multiaxial loading. In the analysis a surface crack under complex combined loading was assumed to be equivalent to a Mode I crack under biaxial loading.

The predictions of critical plane directions, *S-N* curves and fatigue limits are in good agreement with the results of the fatigue tests conducted under in-phase and 90º out-of-phase combined tension and torsion loading.

REFERENCES

1. McEvily, A.J., Eifler, D., Macherauch, E. (1991) *Eng Fract Mech* **40**: 571-584.
2. Kitagawa, H., Takahashi, S. (1976) *Proc 2nd Int Conf Mech Behav Mater*: 627-631.
3. Endo, M., McEvily, A.J., Matsunaga, H., Eifler, D. (2006) In: *Proc ECF 16: Fracture of Nano and Engineering Materials and Structures*, Gdoutos, E.E. (Ed.), 411_end.pdf, Springer.